J Mater Sci: Mater Med (2008) 19:1363–1369
DOI 10.1007/s10856-007-3263-7

Laser surface processing of Ti6Al4V in gaseous nitrogen: corrosion performance in physiological solution

Raghuvir Singh · S. Ghosh Chowdhury · S. K. Tiwari · Narendra B. Dahotre

Received: 22 May 2006 / Accepted: 14 August 2007 / Published online: 4 October 2007

Abstract Laser surface processing was carried out in gaseous nitrogen atmosphere at ambient temperature. The laser scan speed was varied (50–150 cm/min) at constant power of 1500 watts and resulting changes such as microstructural evolution, hardness, and electrochemical response of modified surface in Ringer's physiological solution at varying pH were studied. Increase in laser scanning speed was found to reduce the thickness of alloyed zone from 258 to 87 μm. The microstructure of laser-modified surface contains dendrites grown perpendicular to the laser traverse direction, beneath which basket weave structure of acicular α (martensite) was prevalent. Hardness at the top surface of laser-processed at 50 cm/min was ∼1137 kg/mm^2 that reduced with increase in the laser scan speed (577 kg/mm^2 at 150 cm/min). Laser surface processing shifted the corrosion potential of Ti6Al4V towards noble side as compared to untreated alloy; the maximum shift by ∼494 mV was recorded in pH ∼ 9 solution. Passivation after laser surface modification was improved as currents were at least 1/3 of the untreated Ti6Al4V in passive region. While the pitting potential of untreated material was found to increase from 1.84 V for 4.0 pH to >2.5 V for 9.0 pH, the pitting potential after laser treatment was observed to drop from maximum of 74% for 4.0 pH (at 100 cm/min) to maximum of 42% for 9.0 pH (at 150 cm/min).

R. Singh · S. G. Chowdhury · S. K. Tiwari
National Metallurgical Laboratory, Jamshedpur 831007, India

N. B. Dahotre (✉)
Department of Materials Science & Engineering,
The University of Tennessee, Knoxville, TN, USA
e-mail: ndahotre@utk.edu

1 Introduction

Titanium alloys are widely sought after materials for biomedical applications, as they possess better corrosion resistance and biocompatibility as compared to stainless steel, Co-Cr alloys [1–2]. Among various titanium alloys, Ti6Al4V is extensively used due to its useful mechanical and electrochemical properties. Lately, vanadium, a constituent of this alloy, has been reported to cause undesirable biological reactions [3–5]. Electrochemical and corrosive wear in the physiological solution caused release of metallic ions including vanadium from implant in the patient [6–7]. Despite their good corrosion resistance, metal ions from Ti6Al4V implants are highly probable due to two important reasons: (i) destruction of passive film due to scratching by hard tissues during movements and low repassivation rate resulted in delay of film repair on the surface [5], (ii) poor tribological properties of Ti6Al4V which can enhance both wear debris/metal particle and accelerate the corrosion reaction of implant [8–10].

Potential of surface modification has been recognized these days to improve the metal/alloy surface to enhance the interfacial properties for accelerated implant-host response [11–14]. Various surface modification methodologies such as plasma ion implantation [11, 15–16], laser melting [17–20] and laser surface alloying [21–29], physical and chemical vapor deposition (PVD and CVD) [30–31], thermal oxidation [32], electrochemical surface modification/anodizing [33], have been tried out to improve wear, corrosion, and fretting resistance of orthopaedic implant materials including Ti6Al4V. The surface fabricated by nitrogen-ion beam implantation and plasma nitriding has been shown to be either beneficial or detrimental to the fatigue resistance of titanium alloys [34]. This depends on the treatment conditions including

temperature. Plasma nitriding over short times can produce an improvement, whereas longer process times can be detrimental to fatigue properties [34]. Pitting corrosion resistance of Ti6Al4V alloy after implantation by calcium and silicon ions was shown to deteriorate [35]. The delamination and failure of a TiN coating produced by CVD on the articulating surfaces of Ti-alloy orthopaedic implants have been observed in in-vitro wear simulations and clinical studies [31]. Generally, the coatings produced by CVD and PVD do not provide sufficient adherence to the surface due to limited interaction between substrate and deposit. Thermal oxidation of Ti6Al4V was performed at 500 °C and 700 °C to improve corrosion resistance and biocompatibility of its surface [36]. Osteoblastic cell attachment to the thermally treated surface was shown to improve on the oxide grown at 700 °C, however, its corrosion resistance did not show any improvement in the Ringer's physiological solution. The methods listed above have limitations concerning the performance of tailored surfaces and their complex operating procedures. Plasma based techniques [11, 15–16] and laser treatments [17–29] have been developed and increasingly used to produce tailored surfaces suitable for bio-applications. Lasers though have been used for fabrication operations such as drilling, cutting and welding for a long time they, however, showed significant potential for surface modification in recent years. Both laser surface melting (LSM) and laser surface alloying (LSA) of structural materials showed improvement in their corrosion and tribological properties [17–29]. Alloying/cladding components are, however, limited when intended application is human body; due to sensitivity and non-biocompatibility of biological system to most metal ions. Acceptability of laser alloying of titanium alloys with nitrogen is primarily due to the biocompatibility of the resultant titanium nitride [15, 37], which is desirable for tribological and corrosion resistance of the surface. Some work has been carried out on laser surface alloying with nitrogen that showed significant changes in the performance such as wear and hardness of functional surface [22–24, 25–29]. They have shown cracks in alloyed layer with varied corrosion resistance. Achieving the crack-free surface with optimized laser parameters is still a subject of investigation. As has been shown in our earlier experiments of laser melting of Ti6Al4V and stainless steel 316 L that laser scan speed and laser power can vary the surface properties [19–20, 38]; present study focuses on to laser nitrogen alloying with varying speed to improve corrosion and wear resistance suitable for bio-implant applications. Additionally, the effect of pH on laser-processed Ti6Al4V was investigated as it is being used as an orthopaedic implant, dental screw, in centrifugal blood pump, for surgical equipments where it may encounter a wide range of pH from 4.0–9.0 (in various parts/organ such as blood, urine, saliva, interstitial fluid, perspiration) in the body [39]. The pH may decrease to as low as 4 during the implantation in hard tissues (surgery) that may take long time to return to the normal pH ($\sim$7.4) [13].

This work was carried out to illustrate the effects of laser scan speed on corrosion, microstructure, and hardness of surface of nitrogen alloyed Ti6Al4V. A 2.5 kW Hobart continuous wave Nd:YAG laser was used to alloy the surface of Ti6Al4V with nitrogen. Corrosion performance of laser formed surface was evaluated by anodic polarization in Ringer's physiological solution.

2 Materials and methods

Material selected for this study was Ti6Al4V ELI (%wt Al—5.8%, V—4.2%, O—0.13, H—0.01, C—0.07, Ti—balance) as this has been widely used for biomedical applications.

A 2.5 kW Hobart continuous wave Nd:YAG laser equipped with a fiber optic beam delivery system was employed for laser surface melting. Parallel tracks with partial overlapping ($\sim$15%) were laid with the laser beam focused to a spot size of $\sim$21 mm^2 on the surface of the substrate. Laser beam of power 1,500 W was used over a set of samples at different laser scan speeds and constant working distance. The laser treatment parameters and corresponding sample designations are presented in Table 1. Laser surface melting was carried out in presence of nitrogen cover gas flown over the surface at the flow rate of 6 l/min at ambient temperature.

Polishing of untreated and laser treated Ti6Al4V was performed by first grinding the specimens on a series of grit papers ranging from 240 to 1,200 grit followed by cloth polishing with 0.05 μm size alumina slurry. The etchant to reveal microstructure was prepared by adding 10 ml HF and 5 ml HNO_3 to 85 ml of distilled water at room temperature. Microstructures of untreated and treated specimens were revealed by using a Hitachi 3,500 Variable Pressure scanning electron microscope (SEM). Phase identification was carried out on a Seifert 3003 PTS X-ray diffractometer with CuKα radiations. X-ray diffraction (XRD) analysis was performed on both untreated and laser-processed Ti6Al4V to determine the possible changes in

Table 1 Laser processing parameters

Sample	Laser speed (cm/min)	Laser power (W)
LSA50	50	1500
LSA100	100	
LSA150	150	

phases as a result of laser surface treatment. The microhardness tests on untreated and laser treated Ti6Al4V were performed using Vickers hardness tester (Leica, VMHT Auto make) under l00 g normal load applied for 15 s. The hardness values reported are the average of 6 measurements done each at top, intermediate and base regions.

For electrochemical studies, coupons of $20 \times 20 \times 3$ mm^3 size were cut from the laser treated plates using a TechCut10 abrasive high speed cut-off saw (Allied High Tech Products Inc). As-laser treated specimens were washed in acetone before conducting cyclic polarization studies. These tests were carried out in the Ringer's physiological solutions at three different pH ~4.0, 7.4, and 9.0. This was done to evaluate the effect of pH on laser treated specimens, as pH has been reported to vary during surgery and also widely differs among various parts of the body [39]. Ringer's solution was prepared by adding 9 g/L NaCl, 0.17 g/L $CaCl_2$, 0.42 g/L KCl, and 2.0 g/L $NaHCO_3$ (AR grade chemicals) to distilled water. The pH of the solutions was maintained by adding requisite amount of NaOH or HCl. The solution during cyclic polarization tests was maintained at 37 ± 2 °C to simulate the body temperature. For cyclic polarization tests, specimens were mounted in the epoxy and ensured no crevice formation at the contact surface between epoxy and coupon after the test. The reproducibility of polarization curves was ensured by repeating the test for 3 times. The polarization experiments were carried out by scanning the specimens (towards noble potentials) at 1.67 mV/s from about –200 mV with respect to open circuit potentials (OCP) and reversed the scan from transpassive potential. A saturated calomel electrode (SCE) was used as a reference and graphite as counter electrode. A computer controlled Potentiostat/ Galvanostat (Gamry, USA) was used for these experiments.

3 Result and discussions

3.1 Microstructural characterization

Microstructural characterization was carried out to determine the thickness of the laser-treated surface layer as well as the phase evolution. Changes led by laser processing can be compared with the microstructure of as received Ti6Al4V specimen in Fig. 1a where both α and β are clearly distinguishable with the later rich in vanadium. The microstructures shown in Fig. 1b–d are of laser-processed Ti6Al4V at a various laser scan speeds. The thickness measured at 5 different locations of alloyed zone generated at three different laser scan speeds has been tabulated as a range of variation in Table 2 and may be compared with the Fig 1b–d. Such information related to hardness is important especially from the viewpoint that the intermediate layer has shown the hardness lower than the top but higher than the base substrate and thus this can be indirectly qualitatively correlated with the diffusion and concentration of nitrogen that evolve Ti–N in the top but solid solution (interstitial) within the intermediate layer. Decrease in the thickness of the alloyed zone with increase

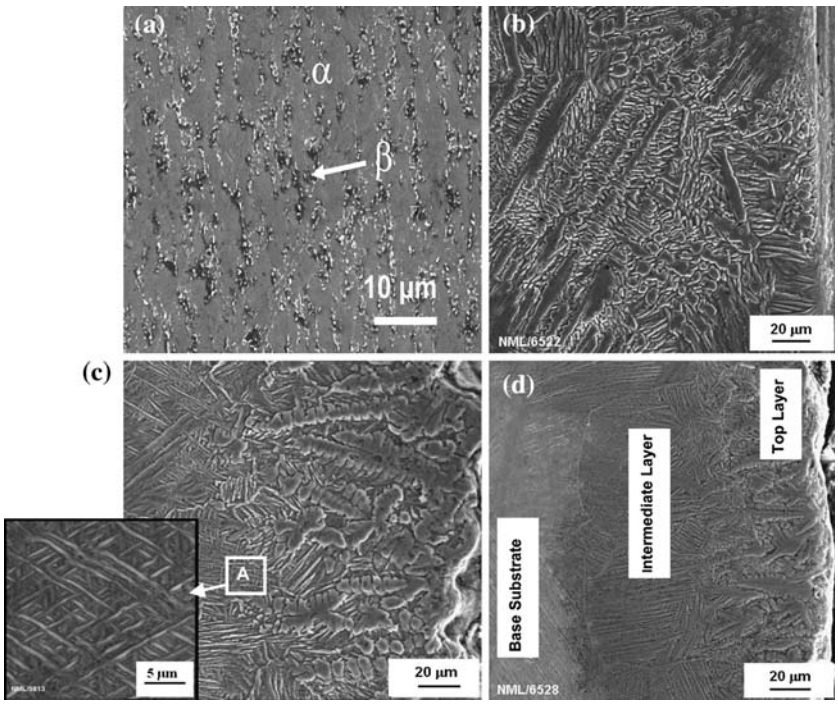

Fig. 1 (**a**) Microstructure of untreated Ti6Al4V (**b**) Microstructure of Ti6Al4V laser-processed at 50 cm/min. (**c**) Microstructure of Ti6Al4V laser-processed at 100 cm/min (**d**) Microstructure of Ti6Al4V laser-processed at 150 cm/min

Table 2 Thickness and vicker hardness of alloyed layer

Sample	Thickness range of alloyed layer (μm)	Hardness at 100 g load (kg/mm^2)		
		Top layer (deviation)	Intermediate layer (deviation)	Base (deviation)
LSA50	253–263	1137 (± 16)	438 (± 9)	279 (± 8)
LSA100	162–172	645 (± 13)	513 (± 12)	
LSA150	82–92	577 (± 19)	443 (± 8)	

in laser scan speed can be related to the lesser quantity of molten/alloyed (reacted material) volume produced due to the decrease of laser residence (interaction) time. The microstructures (Fig. 1b–d) clearly show the dendritic layer in the top portion of the laser-resolidified region at all scan speeds. Dendrites are grown perpendicular to the laser scan direction. The arms of the dendrite were found to be of ~5 μm long and reduced to ~2.5 μm with increase in speed. Basket weave structure (location A in Fig. 1c), below the dendritic layer (intermediate layer in Fig. 1c) was prevalent in almost all laser-processed specimens, which is associated with the distortion of lattice by interstitial nitrogen [40]. The diffusion coefficient being a temperature dependent physical property, the changes in temperature from the top surface region (during laser melting at the surface) to the regions below surface, the diffusion and hence the concentration of nitrogen gradually lowered at distances from the top surface. At the top surface region, since occurrence of nitrogen is higher than its solubility limit in the Ti-alloy, second phase Ti–N compounds are evolved, however, within the regions below the top surface (containing dendrites), due to the low concentration (below the solubility limit) nitrogen tend to go to the interstitial positions thereby distorting the original lattice structure that is associated with formation of a 'Basket weave' structure.

X-ray diffraction studies are carried out to ascertain different phases present in the nitrided layer. The XRD are presented in Fig. 2. The spectrum for untreated Ti6Al4V indicated the presence of only phases α-Ti and β-Ti. On the contrary, the samples laser surface processed in nitrogen environment, indicated the formations of Ti–N phases such as TiN and $Ti(NO_3)_x$. In general, the intensities of the peaks corresponding to Ti–N phases were observed to decrease (Fig. 2) with increase in laser scan speed (decreased interaction time). The higher intensity, which is an indication of concentration of the phase, at lower laser traverse speed is due to longer residence time of the laser beam on the surface that in turn expected to assist in longer interaction between nitrogen and titanium for formation of more amount of Ti–N phases.

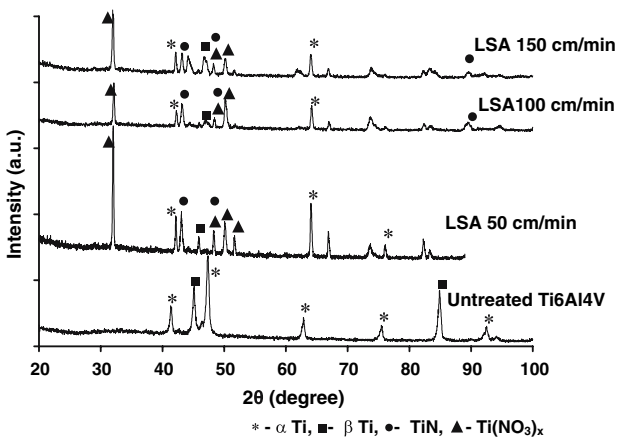

Fig. 2 The XRD pattern of untreated and laser-processed Ti6Al4V

Considerable increase in the hardness of the top layer of laser processed sample, particularly at 50 cm/min (~4 times the untreated Ti6Al4V) was observed which decreased on approaching towards the base material (Table 2). Hardness of the top functional surface decreased from 1137 to 577 kg/mm^2 with increase in the laser scan speed, This can be explained on the basis of short interaction time at high scan speed and, therefore, lower nitrogen concentration available to form probably due to reduced amount of hard nitride phase. The hardness at the top surface is related to the evolution of TiN phase. Further, the lower amount of nitrogen diffused into the alloy (beneath top surface) due to decrease in the diffusion coefficient across thickness [41], which had resulted in the nitrogen-diluted phase (interphase intermediate layer) with lower hardness at the intermediate region. The nitrogen dilution in the intermediate region though resulted in hardness lower than the top (Ti–N containing region) but remained higher than the base substrate.

3.2 Electrochemical response

Laser treatment caused the corrosion potential (E_{corr}) of Ti6Al4V to shift towards nobler (anodic) direction, in Ringer's solution of different pH. This is shown in Table 3 and Figs. 3a–c. The E_{corr} of untreated specimen becomes more active with increase in pH (more alkaline). This can be explained due to variations in redox potential of oxygen (present in the solution) with pH, according to the following equation

Table 3 Electrochemical parameters of untreated and laser-processed Ti6Al4V

pH	4.0			7.4			9.0		
Sample	E_{corr} V	E_{pit} V	I_{pass} μa/cm^2	E_{corr} V	E_{pit} V	I_{pass} μa/cm^2	E_{corr} V	E_{pit} V	I_{pass} μa/cm^2
Untreated	+0.263	+1.84	~13	–0.115	+2.20	20	–0.375	> +2.5	~15
50 cm/min	+0.309	+1.39	3.8	+0.086	~+1.28	6	+0.100	+1.13	~3
100 cm/min	+0.273	+1.37	~4.0	–0.031	~+1.27	5	+0.119	+1.05	< 2
150 cm/min	+0.291	+1.42	< 2	–0.006	+1.0	1.2	–0.062	+1.05	6

Note: The maximum deviation in measuring the potentials (E_{corr} and E_{pit}) was 7%, and the current (I_{pass} and I_{pit}) was 5%

$$^1/_2\ O_2 + 2H^+ + 2e \rightarrow\ H_2O$$

where Nernst equation E(V) = 1.23–0.059 pH is pH dependent.

It is clear from this equation that the increase in pH will result in the more active (negative) redox potential of oxygen–reduction that governs the corrosion kinetics in such solutions. Active redox potential of oxygen–reduction will shift the corrosion potential of Ti6Al4V in more negative direction as were observed from the experimental values (Table 3). After laser treatment, E_{corr} becomes more positive than the base substrate; highest being at the pH—4 than at 7.4 or 9, indicating the variation in the electrochemical behavior of passive film on Ti6Al4V as a result of laser modification. This may be due to the noble nature of titanium nitride (TiN) formed by laser processing (in nitrogen gas) on the surface of Ti6Al4V that exhibited more anodic E_{corr} than the untreated alloy.

Anodic polarization in Figs. 3a–c showed that both untreated and laser-processed Ti6Al4V are under passivation at open circuit conditions. The laser-processed Ti6Al4V showed significantly low passive current as compared to untreated one (Table 3). After laser treatment, passive currents were less than at least 1/3 the untreated Ti6Al4V. This observation was found true at all pH values of Ringer's solution. Passivation current did not show any specific trend with laser scan speed but at pH ~7.4 where it was decreased from 6 to 1.2 μA/cm^2 with increase in laser scan speed (from 50 to 150 cm/min). Passive region at pH ~7.4, though, corrodes at higher rate than at pH ~4.0 or 9.0.

Untreated Ti6Al4V is highly resistant to pitting corrosion as shown by its high pitting potential (E_{pit}) in Ringer's solution and, therefore, is not expected to suffer from pitting attack while in the body. Pitting potential of untreated alloy enhanced from ~+1.84 V (at pH 4.0) to ~+2.5 V (at pH 9.0). The E-pH diagram for Ti–H_2O system at 37 °C (without Cl^- containing solution) showed the presence of passive film, TiO_2 which is responsible for passivation and thereby pitting resistance of this alloy, remains stable over a wide range of pH (from pH ~2 to 14) [42]. The corrosion behavior of titanium, therefore, may be expected to remain unchanged in water at 37 °C. The presence of Cl ions in the above system (as in present situation), however, may disrupt the TiO_2 film consequently producing localized solution chemistry (such as strong acidic with high Cl^- concentration) favorable for pitting corrosion. In the lower pH solutions (~4.0), such aggressive conditions may easily be attained to lead early break down (lower pitting potential) of passive film compared to that in the alkaline solutions. The pitting potential of untreated material was found to increase from 1.84 to 2.5 V with increase in pH. Decrease in pitting potential, an indicative of reducing pitting corrosion resistance, after laser surface processing of Ti6Al4V (Table 3) may be ascribed to the discontinuous TiN film formation and surface roughness induced by laser processing. Slight decrease in pitting potential with increase in laser speed was observed at pH ~7.4 and 9. Current density sharply increases above pitting potential for both untreated and laser-processed coupons, which may be associated with the dissolution of Al in α phase [39]. This is beyond the region of interest for implants made from Ti6Al4V, as the electrochemical potential in-vivo for this alloy is reported to be +500 ± 50 mV (SCE) [43].

Remarkably low corrosion rate, as indicated by the small I_{pass} values of laser-treated Ti6Al4V, as compared to the untreated will result in significantly reduced quantity of metal ions released from the implants. This together with the high hardness (or high wear resistance) of laser-treated Ti6Al4V will further enhance its usefulness, in terms of suppressed inflammatory and undesirable biological reactions resulting from the released metal ions in the body, over the other bio-metallic materials including untreated Ti6Al4V.

The corrosion resistance of nitrogen ion implanted Ti6Al4V was reported to depend on nitrogen doses [44]. The optimum dose of nitrogen was observed (7×10^{16} ions/cm^2) for the best corrosion resistance. The improvement in the passive film resistance, as observed in the present laser-treated Ti6Al4V, was also reported after nitrogen ion implantation [45]. The shallow penetration depth of coating from ion implantation method (0.1–

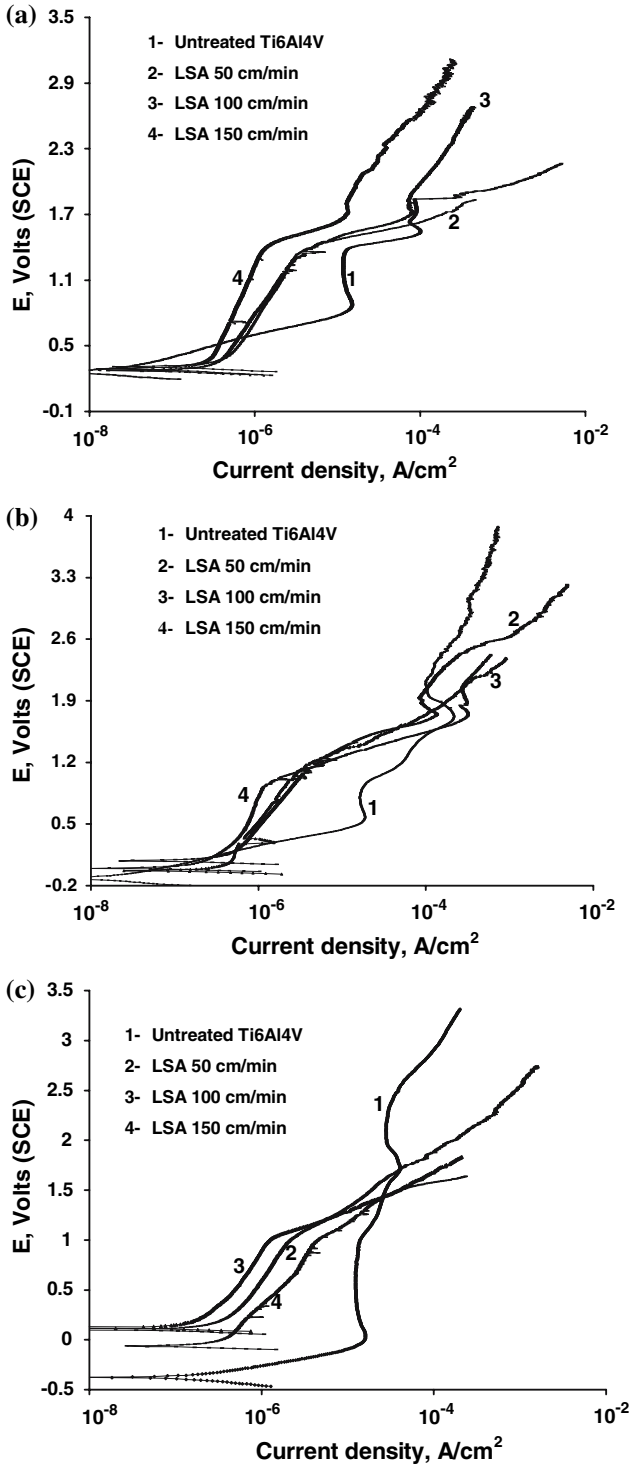

Fig. 3 Anodic polarization curves of Ti6Al4V in Ringer's solution of pH (**a**) 4.0, (**b**) 7.4, and (**c**) 9.0

0.3 μm) may, however, limit its utility for long-term applications. The delamination of coating obtained from CVD and PVD, porosity and adhesion from plasma spraying and high velocity oxy fuel spraying (HVOF) are major concerns for their applications to obtain a corrosion resistant coating [31]. The laser-treatment, results in alloying of the surface, may overcome adhesion and delamination that are the common reasons of coating failure.

4 Conclusions

Laser processing of Ti6Al4V in nitrogen gas has induced dendrite structure on the top surface followed by basket weave acicular α in the intermediate zone. This has increased the substrate hardness (279 H_V) to as high as ~1137 H_V (at 50 cm/min).

Increase in laser scanning speed reduced the thickness of alloyed zone from 258 to 87 μm and hardness from 1137 kg/mm^2 (at 50 cm/min speed) to 577 kg/mm^2 (at 150 cm/min speed).

Laser surface processing shifted the corrosion potential of Ti6Al4V to nobler direction; the maximum shift observed was ~484 mV in solution of pH ~9. Passivation after laser surface modification was improved as currents were at least 1/3 the untreated Ti6Al4V alloy. The pitting potential, however, was reduced after laser-processing.

Acknowledgements A part of this work has been carried out during the BOYSCAST fellowship program at the Department of Materials Science & Engineering, the University of Tennessee, TN, USA. One of the authors (RS) acknowledges the financial support received from DST, Government of India, for this fellowship. Authors also acknowledge the Director, National Metallurgical Laboratory, Jamshedpur, India for granting permission to publish this paper.

References

1. D. M. BRUNETTE, P. TENGVALL, M. TEXTOR and P. THOMSEN, *Titanium in Medicine: Material Science*, Surface Science, Engineering, Biological Responses and Medical Applications, Springer, New York, 2001, p. 25
2. M. NIINOMI, *Metall. Mater. Trans.* **A33** (2002) 477
3. J. BLACK, *J. Bone and Jt. Surg.* **70B** (1988) 517
4. K. L. WAPNER, *Clin. Orthop.* **271** (1991) 12
5. J. R. GOLDBERGA and J. L. GILBERTB, *Biomaterials* **25** (2004) 851
6. S.G. STEINEMANN, Evaluations of Biomaterials, edited by G. D. Winter, J. L. Lray and K. De Groot, John Willey and Sons, 1980
7. M. METIKOS-HUKOVIĆ, A. KWOKAL and J. PILJAC, *Biomaterials* **24** (2003) 65
8. R. A. BUCHANAN, E. D. RIGNEY and J. M. WILLIAMS, *J. Biomed. Mater. Res.* **21** (1987) 367
9. U. I. THOMANN and P. J. UGGOWITZER, *Wear* **239** (2000) 48
10. A. ZHECHEVA, W. SHA, S. MALINOV and A. LONG, *Surf. Coat. Technol.* **200** (2005) 2192
11. P. K. CHU, J. Y. CHEN, L. P. WANG and N. HUANG, *Mater. Sci. Eng.* **R36** (2002) 143
12. U. KAMACHI MUDALI, T. M. SRIDHAR and BALDEV RAJ, *Sadhana* **28** (2003) 601
13. T. HANAWA, *Mater. Sci. Eng.* **A267** (1999) 260

14. N. B. DAHOTRE and A. KURELLA, *J. Biomater Appl.* **20** (2005) 5
15. S. MANDL and B. RAUSCHENBACH, *Surf. Coat. Technol.* **156** (2002) 276
16. H. SCHMIDT, C. KONETSCHNY and U. FINK, *Mater. Sci. Technol.* **14** (1998) 592
17. H. BADEKAS, C. PANAGOPOULOS and S. ECOMNOMOU, *J. Mater. Process. Technol.* **44** (1994) 54
18. T. M. YUE, J. K. YU, Z. MEI and H. C. MAN, *Mater. Lett.* **52** (2002) 206
19. R. SINGH and N. B. DAHOTRE, *Surf. Eng.* **21** (2005) 297
20. R. SINGH, A. KURELLA and N. B. DAHOTRE, *J. Biomater. Appl.* **21** (2006) 49
21. R. A. SILVA, M. A.BARBOSA, R. VILAR, O. CONDE, M. CUNHA and I. SUTHERLAND, *J. Mater. Sci.: Mater. Med.* **5** (1994) 353
22. V. M. WEERASINGHE, D. R. F. WEST and J. D. DAMBORENEA, *J. Mater. Process. Technol.* **58** (1996) 79
23. I. GRACIA and J. D. DAMBORENEA, *Corros. Sci.* **40** (1998) 1411
24. T. M. YUE, T. M. CHEUNG and H. C. MAN, *J. Mater. Sci. Lett.* **19** (2000) 205
25. Z. SUN, I. ANNERGREN, D. PAN and T. A. MAI, *Mater. Sci. Eng.* **A345** (2003) 293
26. P. JIANG, X. L. HE, X. X. LI, L. G. YU and H. M. WANG, *Surf. Coat. Technol.* **130** (2000) 24
27. M. S. SELAMAT, T. N. BAKER and L. M. WATSON, *J. Mater. Process. Technol.* **113** (2001) 509
28. E. GYORGY, A. PEREZ DEL PINO, P. SERA and J. L. MERENZA, *Surf. Coat. Technol.* **173** (2003) 265
29. H. C. MAN, N. Q. ZHAO and Z. D. CUI, *Surf. Coat. Technol.* **192** (2005) 341
30. M. K. LEI and Z. L. ZHANG, *J. Vac. Sci. Technol.* **A15** (1997) 421
31. M. K. HARMAN, S. A. BANKS and W. A. HODGE, *Clin. Orthopaed. Related Res.* **392** (2001) 383
32. M. C. GARCIA-ALONSO, L. SALDANA, G. VALLES, J. L. GONZALEZ-CARRASCO, J. GONZALEZ-CABRERO, M. E. MARTINEZ, E. GIL-GARAY and L. MUNUERA, *Biomaterials* **24** (2003) 19
33. B. YANG, M. UCHIDA, HYUN-MIN KIM, X. ZHANG and T. KOKUBO, *Biomaterials* **25** (2004) 1003
34. A. D. WILSON, A. LEYLAND and A. MATHEWS, *Surf. Coat. Technol.* **114** (1999) 70
35. J. BASZKIEWICZ, M. KAMIIŃSKI, J. KOZUBOWSKI, D. KRUPA, K. GOSIEWSKA, A. BARCZ, G. GAWLIK and J. JAGIELSKI, *J. Mater. Sci.* **35** (2000) 767
36. S. N. MASSOUD, J. B. HUNTER, B. J. HOLDSWORTH, W. A. WALLACE and R. JULIUSSON, *J. Bone Joint Surg.* **79B** (1997) 603
37. A. SCARANO, M. PIATTELLI, G. VRESPA, G. PETRONE, G. IEZZI and A. PIATTELLI, *Clin. Implant Dent. Relate. Res.* **5** (2003) 103
38. R. SINGH and N. B. DAHOTRE, *J. Mater. Sci.* **40** (2005) 5619
39. K. J. BUNDY, *Crit. Rev. Biomed. Eng.* **22** (1994) 139
40. A. B. KLOOSTERMAN and J. TH. DE HOSSON, *J. Mater. Sci.* **32** (1997) 6201
41. B. S. YILBAS and S. Z. SHUJA, *Surface Eng.* **16** (2000) 519
42. S. Y. YU and J. R. SCULLY, *Corrosion* **53** (1997) 965
43. T. P. HOAR and D. C. MEARS, *Proc. Roy. Soc.* A **294** (1966) 486
44. T. SUNDARARAJAN, U. K MUDALI, K. G. M. NAIR, S. RAJESWARI and M. SUBBAIYAN *Anti-Corros. Methods Mater.* **45** (1998) 162
45. L. THAIR, U. K. MUDALI, N. BHUVANESWARAN, K. G. M. NAIR and R. ASOKAMANI, *Corros. Sci.* **44** (2002) 2027